

Table 8: Case 2b: Parameters with Fixed H for Gas Phase Tracer Experiments with NDG Measurements for Gas Holdup at Upper Detector Levels

Run No.	$U\bar{J}_G$ cm/s	Gas Holdup	D_L cm^2/s	Det. Lev.	H	Parameters	
						D_G cm^2/s	K_{La} s^{-1}
14.6-1	255.3	0.42	4696	5	5.86	6059	0.35
		0.45		6		5950	0.33
		0.50		7		5504	0.13
14.6-2		0.42		5	5.86	5805	0.71
		0.45		6		5755	0.47
		0.50		7		4825	0.15
14.7-3	144.3	0.37	3052	5	5.86	2416	0.22
		0.39		6		2472	0.21
		0.41		7		1916	0.14
14.7-4		0.37		5	5.86	2403	0.21
		0.39		6		2399	0.17
		0.41		7		2306	0.23
14.8-5	366.0	0.41	5925	5	8.11	9621	2.63
		0.44		6		8325	1.54
		0.46		7		6720	0.832
14.8-6		0.41		5	8.11	9088	3.32
		0.44		6		7710	1.85
		0.46		7		6970	0.84

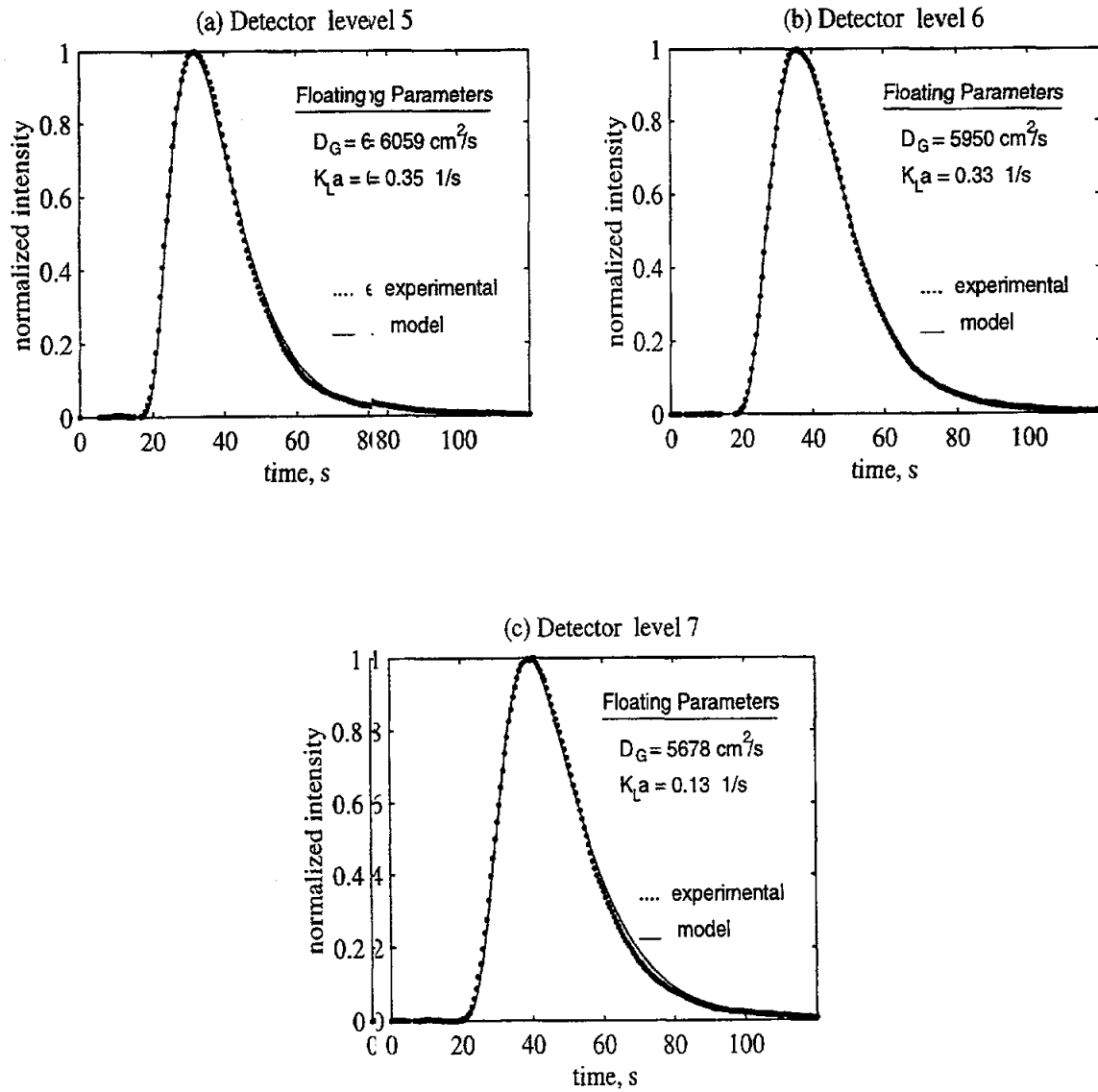


Figure 9: Gas Phase Impulse Response for Run 14.6-1, Injection Time 12.6s

5.2.3 Case 3: Model with Three Floating Parameters: ϵ_G , D_G and K_La

In order to find out what the model predicts as average gas holdup, the data are fitted with the other choice of three parameters by floating ϵ_G , D_G and K_La , and fixing H at its thermodynamic value. As one would expect the fits are very good. The values for the obtained parameters are shown in Table 9. The estimated values of ϵ_G are higher than those measured by DP. The discrepancy is larger in the upper part of the column than at the lower level, but exists for the lower portions of the column as well. For some cases in runs 14.7 and 14.8, the estimated holdup values are larger than both DP and NDG measured values! Therefore, little can be said about the D_G and K_La values from this case of parameter estimation, unless we can independently confirm a pronounced axial solids concentration profile which would have affected the measured gas holdup profiles.

5.2.4 Case 4: Model with Three Floating Parameters: D_G , K_La and α

In the analysis done so far for the gas phase tracer experiments, the tracer concentration $C_i(t, z)$ was assumed to be given by Equation 7. This relationship holds if one assumes no cross-sectional variation of tracer and gas holdup (as considered by the one-dimensional model). However, in reality there is a radial variation of the gas holdup profile (Hills, 1977; Kumar et al., 1994). This affects the measurement of the total argon tracer concentration because the detector gets its major source of radiation from the tracer close to the wall. If the phase holdups and concentrations C_G and C_L are uniform through out the cross section, then the total concentration of tracer is the average of the gas and liquid phase concentrations, weighted by the respective holdups. If, however, the distribution of phases is not cross-sectionally uniform, but has more liquid at the wall, as is the actual case, then the average should not be weighted by the phase holdups, but must also account for the relatively higher contribution of the liquid, due to higher volume fraction of the liquid at the wall. In other words $C_i(t, z) = \alpha \epsilon_g C_G + \epsilon_L C_L$ where $\alpha \leq 1.0$.

It is not possible to know what α is without modeling the radiation received by the detector for a given spatial distribution of the phases and tracer concentration. This in itself is a rigorous and time-consuming procedure. For a preliminary assessment of the effect of an uneven cross-sectional distribution, the model fitting is performed using α as the third floating parameter, instead of ϵ_G or H .

Table 9: Case 3: Parameters for Gas Phase Tracer Experiments with Fixed H

Run No.	U_G c cm/s	H	D_L cm^2/s	Det. Lev.	Model Parameters		
					D_G cm^2/s	ϵ_G	$K_L a$ s^{-1}
14.6-1	25.3	5.86	4696	1	20000	0.20	3.158
				2	6790	0.43	2.495
				3	7879	0.39	1.855
				4	5725	0.43	0.36
				5	7473	0.41	1.45
				6	6256	0.45	0.44
				7	6364	0.49	0.67
14.6-2				1	15000	0.24	4.04
				2	5213	0.46	1.32
				3	6361	0.41	2.19
				4	4317	0.48	0.22
				5	5937	0.43	0.77
				6	5574	0.47	0.33
				7	5246	0.49	0.43
14.7-3	14.3	5.86	3052	1	7340	0.34	0.006
				2	4094	0.39	1.39
				3	4533	0.36	1.58
				4	3628	0.38	0.35
				5	2970	0.42	0.32
				6	2462	0.45	0.16
				7	2426	0.45	0.23
14.7-4				1	5929	0.35	0.006
				2	3329	0.38	0.28
				3	4170	0.34	0.42
				4	2954	0.40	0.16
				5	2553	0.42	0.18
				6	3111	0.44	0.13
				7	2606	0.46	0.14
14.8-5	336.0	8.11	5925	1	20000	0.20	1.80
				2	7235	0.46	0.20
				3	7963	0.43	0.29
				4	7425	0.49	0.10
				5	7320	0.49	0.17
				6	7135	0.51	0.10
				7	6689	0.52	0.08
14.8-6				1	20000	0.22	1.58
				2	9442	0.39	0.28
				3	9800	0.38	0.34
				4	8518	0.46	0.09
				5	7027	0.49	0.12
				6	6580	0.51	0.09
				7	7079	0.54	0.15

Table 10: Case 4: PParameters for Gas Phase Tracer Experiments

Run No.	$U\bar{U}_G$ cmn/s	Gas Holdup	D_L cm^2/s	Det. Lev.	Model Parameters		
					D_G cm^2/s	$K_L a$ s^{-1}	α
14.6-1	25.5.3	0.39	4696	1	9800	0.08	1.0
		0.39		2	7153	2.28	0.198
		0.38		3	7580	2.62	1.00
		0.37		4	5458	0.40	0.22
		0.38		5	7409	0.82	0.17
		0.39		6	6607	0.34	0.07
		0.40		7	6795	0.25	0.00
14.6-2		0.39		1	9800	0.44	1.00
		0.39		2	4854	0.74	0.23
		0.38		3	6428	2.32	0.29
		0.37		4	3763	0.37	0.10
		0.38		5	5863	0.54	0.11
		0.39		6	5729	0.29	0.07
		0.40		7	5544	0.23	0.00
14.7-3	14.4.3	0.34	3052	1	4949	0.64	1.00
		0.33		2	4678	0.78	0.15
		0.32		3	5026	0.99	0.16
		0.32		4	3697	0.35	0.15
		0.33		5	3216	0.30	0.00
		0.34		6	2467	0.16	0.00
		0.35		7	2274	0.12	0.00
14.7-4		0.34		1	4283	0.51	1.00
		0.33		2	3113	0.29	0.30
		0.32		3	4143	0.40	0.38
		0.32		4	2571	0.26	0.15
		0.33		5	2343	0.29	0.04
		0.34		6	2661	0.16	0.00
		0.35		7	2499	0.12	0.00
14.8-5	36.6.0	0.38	5925	1	17470	0.14	1.00
		0.37		2	6007	0.43	0.20
		0.37		3	7216	0.44	0.25
		0.37		4	5135	0.28	0.12
		0.37		5	6025	0.30	0.06
		0.38		6	5671	0.24	0.04
		0.38		7	5863	0.22	0.02
14.8-6		0.38		1	18973	0.11	1.0
		0.37		2	8893	0.37	0.38
		0.37		3	9740	0.38	0.42
		0.37		4	5873	0.23	0.17
		0.37		5	4722	0.28	0.08
		0.38		6	4362	0.22	0.05
		0.38		7	7151	0.23	0.05

Again, the fits are good for all conditions. The parameters are reported in Table 10. There is a distinct trend in the values of α , which is zero at the upper detector levels, and increases with a decrease in height. Such low values of α at the higher levels suggest that the detectors at these levels see only the liquid and no gas. These results can have meaning only if this can be verified.

In order to verify the validity of the results in Case 4, the radiation detected by a detector is modeled by accounting for the cross-sectional variation of gas holdup in the column. Details of this calculation are shown in Appendix II. Once an estimate of C_G and C_L is obtained from the model, it is used in the radiation model to calculate the total concentration C_t .

Figure 10 shows the result of fitting the model response to the experimental data for detector level 7 of Run 14.6-1. The fit is similar to the case shown in Figure 8g, for the case of two-parameter fitting, using holdup estimates from DP measurements. This implies that the total tracer concentration C_t resulting from the radiation calculation is approximately the same as defined by Equation 7. The results of Case 4, with $\alpha \sim 0$, are therefore not valid. The reason for this is that the concentration of tracer in the liquid phase is so low that the influence of high liquid holdup at the wall is offset by the low liquid tracer concentration (refer to Figure 11 and Figure A.2.2 in Appendix II). As seen in Figure A.2.2, the contribution of radiation at these low concentrations of liquid tends to become more uniform across the cross-section, and hence, the effect of the assumed radial gas holdup profile on the results is not very significant. This justifies the use of Equation 7 for this specific gas tracer of low solubility.

So far we have considered a combination of D_G , $K_L a$, H , and ϵ_G as the floating parameters of the model. For Cases 1, 3 and 4, where three floating parameters are used, the fits are good, but the values of H , ϵ_G and α for the respective cases do not compare well with corresponding values from independent measurements (or methods of estimation). For Case 2, when NDG-based values for the holdup are used, the fits are reasonably good with two floating parameters - D_G and $K_L a$. As discussed earlier, the poor fits obtained when using ϵ_G from DP measurements are due to the differences in the mean residence times between the experimental data and model predicted results.

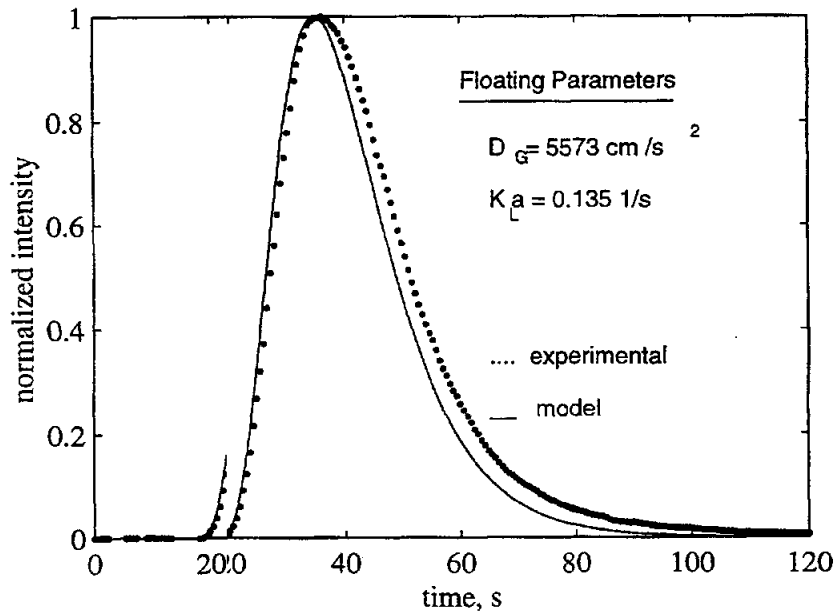


Figure 10: Gas Phase Impulse Response for Run 14.6-1 at Detector Level 7, Injection Time 14.6s (Model 1 Uses Simulation of Incident Radiation)

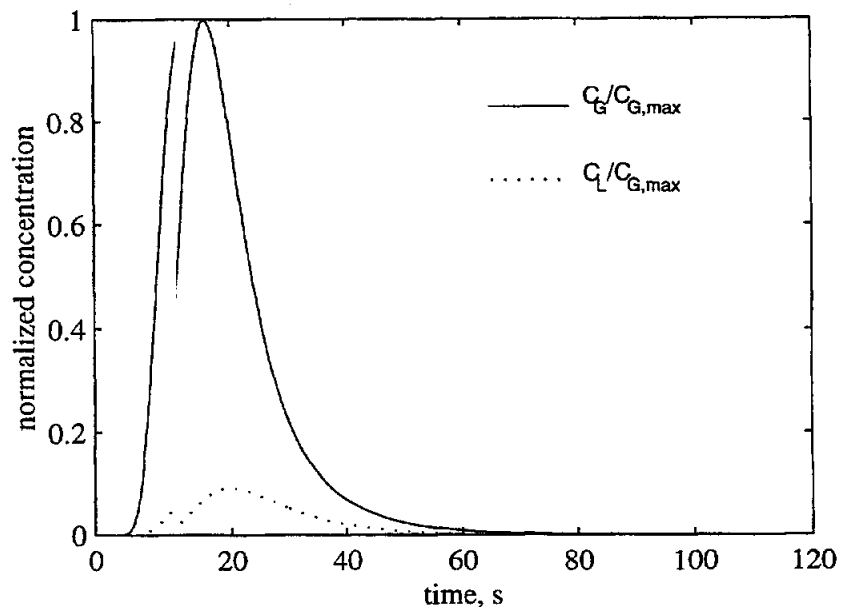


Figure 11: Model Calculated Tracer Concentration in Gas and Liquid Phase (Run 14.6-1 Detector Level 7)

5.2.5 Case 5: Model with Changing Gas Flow Rate and two Floating Parameters, D_G and $K_L a$

Due to reaction in the slurry bubble column reactor, there is a reduction in the gas volumetric flow rate. This affects the superficial gas velocity along the length of the reactor. The conversions for the runs considered in this study result in an average reduction of around 18% in the gas flow rate. The axial dispersion model in its present form can not account for the axial variation of U_G . However, for the purpose of this analysis, the reduction in gas flow rate is considered by assuming a linear change (decrease) in U_G with axial position along the column, since the inlet and outlet gas flowrate are known from experimental data. This is just an approximation. Once the U_G at the intermediate axial positions corresponding to the detector levels are evaluated, these values, $U_{G,z}$, are used in the model to predict the tracer distribution at different axial positions, and fit the experimental data. The average value of $U_{G,z}$ at a given axial position can be used; however since the axial profile of $U_{G,z}$ is not known, the present variation in $U_{G,z}$ is considered. Thus, instead of using the inlet gas velocity, as done in Case 2, we now employ the gas velocity estimated at the detector level. The resulting parameters are reported in Table 11. Figure 12 shows the fits of the model to experimental data for Run 14.6 - 1. For this case, with only two floating parameters, the fits are much better than for Case 2 (using DP measurements for ϵ_G and inlet U_G), although they are not as perfect as for the three floating parameter cases. However, these fits are acceptable, since only two floating parameters are used.

5.2.6 Case 6: Model with three Floating Parameters, D_G , $K_L a$ and U_G

As a final case, regression is performed to fit the experimental data to the model with three floating parameters, a position-dependent superficial gas velocity, $U_{G,z}$, D_G and $K_L a$. This is done in order to estimate the average variation of U_G with axial position z . The resulting fits are as good as the other fits with three floating parameters. The values of the obtained parameters are shown in Table 12. The values of $U_{G,z}$, in general suggest a monotonic decrease of the gas velocity with axial position, especially at the higher detector levels, as expected.

Therefore this set of parameters for D_G , $K_L a$ and U_G , along with the independent estimates of ϵ_G and H , form the most reliable set of parameters. Although three floating parameters used, the values of $U_{G,z}$ obtained are reasonable, and fall within the range of experimental values. This case is therefore the one that should be considered for analysis of the model parameters.

Table 11: Case 5: Parameters for Gas Phase Tracer Experiments (Using Variable U_G)

Run No.	U_G cm/s	Gas Holdup	D_L cm^2/s	Det. Lev.	H	Parameters	
						D_G cm^2/s	$K_L a$ s^{-1}
14.6-1	24.8.82	0.39	4696	1	5.86	9025	0.006
	24.2.29	0.39		2		5310	0.63
	24.6.08	0.38		3		5577	0.28
	23.3.15	0.37		4		4940	0.26
	22.2.29	0.38		5		5433	0.12
	21.1.9	0.39		6		4966	0.13
	21.1.5	0.40		7		4844	0.14
14.6-2	24.8.82	0.39		1	5.86	7599	0.006
	24.2.29	0.39		2		4908	1.56
	24.6.08	0.38		3		4677	0.46
	23.3.15	0.37		4		3937	0.57
	22.2.29	0.38		5		4457	0.19
	21.1.9	0.39		6		4604	0.14
	21.1.5	0.40		7		4154	0.18
14.7-3	14.4.0	0.34	3052	1	5.86	5000	3.52
	13.3.6	0.33		2		3410	0.78
	13.3.4	0.32		3		2583	0.42
	12.2.7	0.32		4		3156	0.35
	12.2.2	0.32		5		3017	0.40
	11.1.8	0.33		6		2990	0.51
	11.1.7	0.33		7		2100	0.28
14.7-4	14.4.0	0.33		1	5.86	5500	3.52
	13.3.6	0.33		2		3261	0.50
	13.3.4	0.32		3		2762	0.29
	12.2.7	0.32		4		2871	0.33
	12.2.2	0.32		5		2928	0.43
	11.1.8	0.33		6		2982	0.39
	11.1.7	0.33		7		2867	0.35
14.8-5	35.5.3	0.38	5925	1	8.11	13922	0.002
	34.4.4	0.37		2		8413	1.70
	34.4.0	0.37		3		7894	0.78
	32.2.5	0.37		4		6584	0.57
	31.1.0	0.37		5		6559	0.50
	30.0.1	0.38		6		5777	0.36
	29.9.6	0.38		7		5309	0.22
14.8-6	35.5.3	0.38		1	8.11	16533	0.002
	34.4.4	0.37		2		8691	0.27
	34.4.0	0.37		3		9119	0.25
	32.2.5	0.37		4		7325	0.28
	31.1.0	0.37		5		5792	0.40
	30.0.1	0.38		6		5108	0.29
	29.9.6	0.38		7		5765	0.30

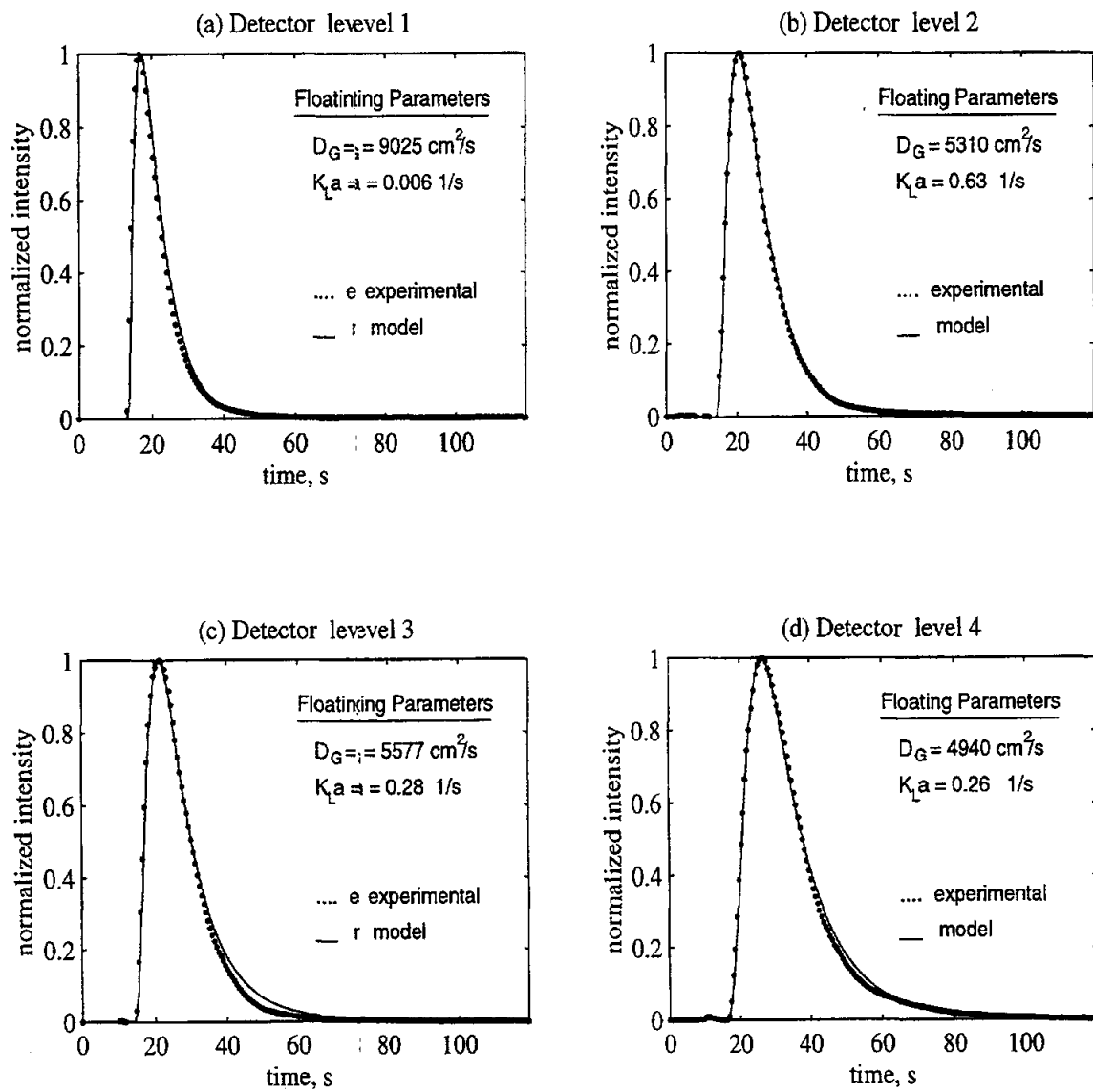


Figure 12: Gas Phase Impulse Response for Run 14.6-1 using Position Dependent Superficial Gas Velocity, Injection Time 12.6s

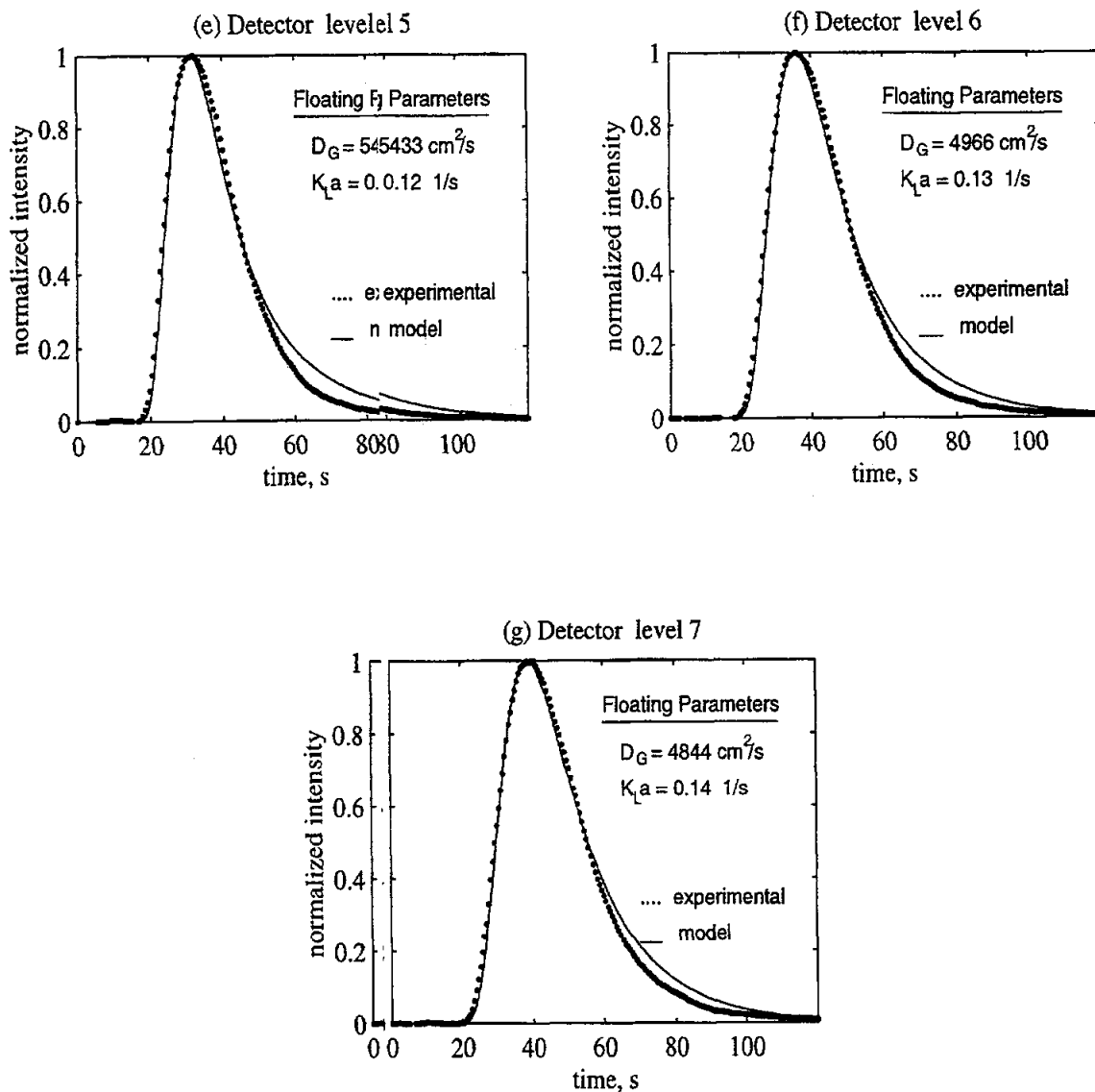


Figure 12 (contd.): Gas PPhase Impulse Response for Run 14.6-1 using Position Dependent Superficial Gas Velocity, Injection Time 12.6s

Table 12: Case 6: : Parameters for Gas Phase Tracer Experiments

Run No.	U_G cm/s	Gas Holdup	D_L cm^2/s	Det. Lev.	Model Parameters		
					D_G cm^2/s	$K_L a$ s^{-1}	U_G cm/s
14.6-1	225.3	0.39	4696	1	9800	0.008	25.3
		0.39		2	6907	0.60	24.8
		0.38		3	6970	1.05	25.3
		0.37		4	5282	0.45	23.9
		0.38		5	6974	0.36	24.4
		0.39		6	5817	0.49	23.4
		0.40		7	5885	0.51	22.7
14.6-2		0.39		1	9800	0.001	25.3
		0.39		2	4536	0.99	24.1
		0.38		3	6239	0.63	25.0
		0.37		4	3717	0.44	22.8
		0.38		5	5500	0.23	23.8
		0.39		6	5173	0.42	23.2
		0.40		7	4798	0.53	22.6
14.7-3	114.3	0.34	3052	1	4345	0.23	14.3
		0.33		2	3104	0.36	13.3
		0.32		3	4082	0.44	13.9
		0.32		4	3449	0.43	13.2
		0.33		5	2714	0.47	12.4
		0.34		6	2133	0.33	12.1
		0.35		7	2157	0.43	12.0
14.7-4		0.34		1	3627	0.18	14.3
		0.33		2	3104	0.36	13.3
		0.32		3	4081	0.44	13.9
		0.32		4	2647	0.29	12.8
		0.33		5	2230	0.34	12.4
		0.34		6	2286	0.34	12.1
		0.35		7	2288	0.31	11.9
14.8-5	336.0	0.38	5925	1	16150	0.003	36.0
		0.37		2	6250	0.51	32.7
		0.37		3	7205	0.54	33.3
		0.37		4	6127	0.21	30.9
		0.37		5	6226	0.45	30.6
		0.38		6	5722	0.33	30.0
		0.38		7	5348	0.30	29.9
14.8-6		0.38		1	19247	0.002	36.0
		0.37		2	9044	0.37	34.9
		0.37		3	9660	0.50	35.0
		0.37		4	7281	0.15	31.3
		0.37		5	5636	0.32	30.6
		0.38		6	5092	0.28	30.0
		0.38		7	5868	0.35	29.9

5.2.7 Discussion of Results

The parameters that truly need to be estimated from this model, are the gas phase dispersion coefficient LD_G and the gas-liquid mass transfer coefficient K_La . For the sake of analysis of these model parameters, and to study their dependence on superficial gas velocity, the means and standard deviations of D_G and K_La at each process rate are calculated and reported in Tables 13 and 14 for all the cases that have been considered in this study. The averages are calculated for both trials of each run, excluding the parameters obtained by fitting the response of the lowest detector.

Table 13: Average D_G at each Process Rate for the Various Cases Studied

Case No.	Run	D_G cm^2/s	σ_G cm^2/s
1	14.6	5637	1305
	14.7	2801	1010
	14.8	4951	1504
2a a	14.6	6601	835
	14.7	2984	873
	14.8	9795	1770
2b b	14.6	5650	446
	14.7	2330	204
	14.8	8072	1155
3 i	14.6	6094	992
	14.7	3236	722
	14.8	7684	1047
4 :	14.6	6098	1019
	14.7	3223	952
	14.8	6388	1301
5 i	14.6	4816	473
	14.7	2910	336
	14.8	6861	1392
6 i	14.6	5649	1022
	14.7	2908	723
	14.8	6621	1437

Except for Case 1, all other cases show an increase in D_G with gas velocity. Case 1 has H as one of the floating parameters. The fitted values of H are considerably lower than their corresponding values from thermodynamics. This may be the reason for this anomaly. In general, there is a very large spread of D_G about the mean value.

Literature correlations for D_G (Mangartz and Pilhofer, 1980; Field and Davidson, 1980; Towell and Ackerman, 1972), reported in Table 15, are valid only for superficial

Table 14: Average $K_{L,a}$ at each Process Rate for the Various Cases Studied

Case No.	Run	$K_{L,a}$ 1/s	σ_k 1/s
1	14.6	1.23	0.81
	14.7	0.91	0.92
	14.8	1.18	0.97
22a	14.6	2.7	2.2
	14.7	1.66	1.00
	14.8	4.19	4.04
22b	14.6	0.358	0.26
	14.7	0.195	0.03
	14.8	1.834	0.99
3	14.6	1.04	0.79
	14.7	0.44	0.50
	14.8	0.161	0.08
4	14.6	0.984	0.99
	14.7	0.349	0.27
	14.8	0.299	0.08
5	14.6	0.413	0.41
	14.7	0.421	0.14
	14.8	0.494	0.41
6	14.6	0.370	0.37
	14.7	0.378	0.06
	14.8	0.359	0.12

gas velocities up to 13 cm/s, which is lower than the range of velocities of interest to us. Therefore a comparison is made only between Run 14.7, which is at the lowest gas velocity, and the correlation predictions from the literature.

The values of D_G predicted by the above correlations are much higher than the mean value of $D_G = 2908 \text{ cm}^2/\text{s}$ at U_G of 14 cm/s obtained in this study. The implications of these results are completely different from those for the liquid phase results, which suggest that an increase in pressure causes an increase in the liquid dispersion coefficients. The correlation equations suggest that an increase in pressure, which increases the holdup, will lower the magnitude of the gas dispersion coefficients. This occurs because the correlations relate the dispersion coefficient to the swarm velocity of the bubbles, which decreases with a decrease in bubble size or an increase in gas holdup. The physical basis for these equations is not completely known. Intuitively it is expected that the presence of an excess of smaller bubbles should only increase the dispersion of the gas as more bubbles follow and recirculate along with the liquid

Table 15: Correlations for Gas Dispersion Coefficient in Bubble Columns

Investigator	Equation (in SI)	Range of Variables	Prediction of D_G at U_G 14 cm/s (cm^2/s)
Towell and Ackerman	$D_G = 199.7 D_C^2 U_G$	$0.00854 \leq U_G \leq 0.13$ m/s $0.0072 \leq U_L \leq 0.0135$ m/s $D_C = 0.406, 1.067$ m	5835
Field and Davidson	$D_G = 56.4 D_C^{1.33} (\frac{U_G}{\epsilon_G})^{3.56}$	$0.00854 \leq U_G \leq 0.13$ m/s $0.0 \leq U_L \leq 0.0135$ m/s $0.076 \leq D_c \leq 3.2$ m	13435
Mangartz and Pilhofer	$D_G = 50.0 D_C^{1.50} (\frac{U_G}{\epsilon_G})^{3.00}$	$0.015 \leq U_G \leq 0.13$ m/s $0.0072 \leq U_L \leq 0.0135$ m/s $0.092 \leq D_c \leq 1.067$ m	11911

phase, while the larger bubbles move up the column. It must be noted that there is also a large variation in the predictions of D_G from correlations. The correlations are shown to have an error of up to 60 %. Therefore, no conclusion regarding D_G can be made based on the comparison with these correlations.

Unlike the consistent trends for the gas phase dispersion coefficients with superficial gas velocity, $K_L a$ values shows no particular pattern (as indicated by the results of ANOVA in Tables A.4.3 and A.4.4 for Cases 1 and 6). In fact the standard deviations indicate the large variation of $K_L a$ from the mean values. This large spread of the data, and the lack of any trend suggests that the model is quite insensitive to $K_L a$. If one looks at these results from Case 5 and Case 6, which are the most reliable cases, it appears that there is no dependence of $K_L a$ on gas velocity. Here again, the spread is significantly large. Unfortunately, there are no existing literature correlations for $K_L a$ under these conditions of pressure and gas velocity, to make any quantitative comparisons.

5.2.8 Conclusions and Future Work

- In general, good fits are obtained with the one-dimensional model using three floating parameters, (D_G , H and $K_L a$), (D_G , $K_L a$ and ϵ_G), (D_G , $K_L a$ and α) and (D_G , $K_L a$ and U_{GG}). Although the fits are good for these cases, there is a mismatch between the model predicted H , ϵ_G and α from the first three cases (1, 3 and 4) and corresponding independent measurements. Only for Case 6 are the fitted values of U_G reasonable and relate well to independent experimental information.

Since independent estimates of all model parameters except D_G and K_La are available, ideally a two floating parameter model should suffice. When such a two parameter model, with D_G and K_La as floating parameters, is used, reasonable fits are possible only when the variation of superficial gas velocity, due to gas consumption, is accounted for. A linear decrease in U_G over the entire dispersion height is considered for this. This demonstrates the importance of accounting for the varying gas velocity in the column, despite the fact that the observed conversions are quite low. In Equation 13, a decrease in U_G is equivalent to an increase in ϵ_G . This explains the results obtained for Cases 2 and 3. Therefore, by accounting for the change in U_G with axial position in the column, the model is able to provide good fits of data when estimates for ϵ_G from DP measurements are used.

A comparison of the results between Cases 5 and 6 shows that the D_G values are about the same.

- In the process of using the various approaches for fitting the data, it is shown (in Case 4) that the assumptions for estimating the total argon concentration, given by Equation 7, are good approximations for the system under consideration.
- The values of the parameters obtained by model fits of experimental data are more consistent for the top two to three detector levels for all the cases considered. At the lower levels the values of D_G start increasing. Based on the dispersion Peclet number, it is seen that the model is most suitable for interpretation of the measurements at the upper levels, where the deviation from plug flow is the smallest.
- A parametric sensitivity is performed for Case 1, with three floating parameters, D_G , H and K_La , by fixing ϵ_G from DP measurements. It is found that the model is most sensitive to Henry's law constant H , and least sensitive to K_La . Due to this, variations in K_La do not affect the model predictions appreciably. It is noted, however, that K_La values of zero cannot be used as the data then simply cannot be fitted by the model. In addition, based on the results for Case 2 and Case 5, where two floating parameters are used, considerable model sensitivity to gas holdup and superficial gas velocity is evident.
- The average values of D_G indicate that D_G increases with superficial gas velocity. Literature correlations predict gas dispersion coefficients much higher in

magnitude than observed in this study. This is thought to be due to the large error involved in the correlations.

While there is a consistent increase in D_G with gas velocity, the increase between runs 14.6 and 14.8, that is, for velocities 25.3 cm/s and 36 cm/s appears only marginal considering the large difference in gas velocities (when compared to the differences between runs 14.7 and 14.6), as seen in Table 13. Run 14.8 is at a lower pressure (3.6MPa) than the other two runs (5.2MPa). This implies that a reduction in pressure causes a lowering of D_G , which for the case of run 14.8 would be expected to be higher at a pressure of 5MPa. However, there is no sufficient experimental information at present to confirm this hypothesis fully.

- While the gas dispersion coefficient seems to show reasonable trends, the volumetric mass transfer coefficient, $K_L a$, shows no pattern. In addition, there are large variations of $K_L a$ about the mean value.

Overall, the dispersion model is able to match the tracer responses in the column. Judging from all the cases for different floating parameters that are studied, it is clear that an accurate estimate of the average gas holdup and superficial gas velocity is absolutely necessary for good fits of data.

With regard to the two main parameters, a large variation in D_G values is obtained at different axial positions of measurement, which shows an increase of D_G with a decrease in height. The $K_L a$ values obtained by fitting the data show no consistent patterns and have a very large spread about their means, which basically indicates that the model is insensitive to $K_L a$. As a result, the effect of U_G on $K_L a$ cannot be properly assessed. This is perhaps also due to the lack of a physical basis for using the axial dispersion model for the fluid dynamic situation in the present column.

A model that better captures the nature of flow in bubble columns and distinguishes between the possibly different bubble sizes is required to consistently predict the characteristics of the tracer responses at all levels in the column. For this purpose, we propose to use the phenomenological Two Phase Recycle with Cross-Flow Model (TRCFM), which accounts for the movement of different bubble classes (gas) within the column and their interaction with the liquid phase. The axial variation of superficial gas velocity and gas holdup can be suitably incorporated into such a model.

6 Gas - Liquid Mixing and Scale-Up Issues in Bubble Columns

In bubble columns liquid recirculation is set up in the column in a time-averaged sense (Devanathan et al, 1990; Hills, 1974). The maximum liquid velocity increases with increasing superficial gas velocity, as the gas holdup increases and the radial holdup profile becomes steeper (Kumar et al, 1994). Simultaneously, due to increased turbulence there is an increase in the radial and axial turbulent diffusivities (Devanathan, 1991; Degaleesan et al. 1995). The effective or overall axial liquid dispersion coefficient is a result of convective and turbulent mixing. The overall liquid axial dispersion coefficient can be tentatively approximated by Taylor diffusivity as

$$D_L = \frac{2\bar{U}_{LU}^2 R^2}{D_{rr}} + D_{zz} \quad (22)$$

where \bar{U}_{LU} is the mean upflow liquid velocity calculated as

$$\bar{U}_{LU} = \frac{\int_0^{R^*} u_{Lz}(r) \epsilon_L(r) r dr}{\int_0^{R^*} \epsilon_L(r) r dr} \quad (23)$$

As U_G increases, \bar{U}_{LU} , D_{rr} and D_{zz} increase. As long as the increase in \bar{U}_{LU}^2 is larger than the increase in D_{rr} , then both terms in Eqn 22 will increase with increasing gas velocity.

We have experimental results for liquid velocities and turbulent diffusivities in smaller diameter columns and lower gas velocities (Degaleesan and Duduković, 1995) velocities. When extrapolated to larger columns, this yields turbulent diffusivities in the range $D_{rr} \sim 100$ to $1500 \text{ cm}^2/\text{s}$, and $D_{zz} \sim 1500$ to $2000 \text{ cm}^2/\text{s}$. The mean upflow velocities can be obtained using the one-dimensional model of Kumar et al. (1994) for liquid velocity. This yields $\bar{U}_{LU} \sim 23$ to 35 cm/s . The above values are calculated for the existing conditions from U_G 14 cm/s to 36 cm/s, respectively. When substituted in Eqn 22, this yields values of D_L to be 3300 to 6100 cm^2/s . It is noted that the expression for Taylor diffusivity is only an approximate one for use in bubble columns. In addition the convective and turbulent parameters are obtained by extrapolation of the existing data for smaller diameter columns. This gives us reasonable results for D_L under the existing operating conditions.

Using the axial dispersion model (ADM) and fitting the model to experimental data, the axial dispersion coefficients for the gas, D_G , and liquid, D_L , have been evaluated from tracer data under methanol synthesis conditions. For the liquid phase,

the relatively larger values of dispersion coefficients obtained, when compared to correlation predictions of liquid dispersion coefficients at atmospheric pressure, are qualitatively justified based on the holdup differences between the two systems. For the gas phase, comparison of the fitted D_G with literature correlations are counter intuitive and opposite to that of the liquid phase experimental results.

It is clear that none of the existing correlations can be used satisfactorily to predict mixing (dispersion coefficients) in the gas or liquid phase under existing conditions. Since the experiments considered here are only for a single column diameter, and since the effect of pressure can not be discerned from these experiments, no correlations can result from the present work. In addition, results of parameter estimation at the various detector levels indicate the effect of L/D ratio on the model parameters, especially at the lower detector levels of the column.

With regard to scale-up to industrial size columns, caution must be exercised in extrapolating the correlations for the dispersion coefficients to large diameter columns.

7 Conclusions

The liquid (slurry) and gas phase tracer data have been interpreted with the one dimensional axial dispersion model (ADM).

For the case of the liquid, the dispersion model is able to give good fits for the detectors that do not exhibit any overshoots. The obtained dispersion coefficients show an increase with gas velocity. However, there is a large scatter in the axial dispersion coefficient obtained at different detector levels, which suggests that the model is inadequate to describe the behavior of the liquid within the entire column with a single dispersion coefficient. For this purpose, we propose to use the Recycle with Cross Flow and Dispersion Model (RCFDM).

For the gas phase tracer analysis, good fits are possible using the ADM at almost all detector levels, but there is a variation in the estimated parameters with detector level. While the gas phase dispersion coefficient shows an increase with gas velocity, no particular dependence is seen with regard to the volumetric mass transfer coefficient. To better represent the flow pattern along with the bubble size distribution and gas-liquid exchange, we propose to use the Two Phase Recycle with Cross Flow model (TRCFM) in the future.

Comparison with literature correlations for the dispersion coefficients shows the lack of any suitable correlations under existing operating conditions. In order to use the correlations for scale-up, additional experiments at different column diameters,